Effects of log *P* and Phenyl Ring Conformation on the Binding of 5-Phenylhydantoins to the Voltage-Dependent Sodium Channel

Milton L. Brown,[†] George B. Brown,[‡] and Wayne J. Brouillette*,[†]

Department of Chemistry and Department of Psychiatry and Behavioral Neurobiology, University of Alabama at Birmingham, Birmingham, Alabama 35294

Received October 4, 1996[⊗]

Binding to the neuronal voltage-dependent sodium channel (NVSC) was evaluated for 12 5-phenylhydantoins which systematically varied either log *P* and/or 5-phenyl ring orientation. The linear correlation of log *P* with in vitro sodium channel binding activity (log IC_{50}) for hydantoins **1**−**12** and diphenylhydantoin (DPH) ($r^2 = 0.638$) suggested that simple partitioning into the lipid phase is important but not sufficient to account for the effects of hydantoins on the NVSC. Comparisons among different hydantoins with the same log *P* but different low-energy phenyl ring orientations revealed that, in addition to log *P*, the correct 5-phenyl orientation is important for efficient binding.

The neuronal voltage-sensitive sodium channel (NVSC) is a transmembrane protein complex[1] which, in concert with other voltage-dependent ion channels, is essential for the generation of action potentials in neurons and other excitable cells.[2−4] Action potentials nominally consist of two phases: (1) depolarization caused by the rapid entry of sodium into the cell through the NVSC and/or calcium entry into the cell through voltage-sensitive Ca^{2+} channels and (2) potassium movement out of the cell through voltage-sensitive K^+ channels, repolarizing the cell and setting the resting membrane potential (−60 mV).[5]

The NVSC can exist in at least three states, and transitions between the states involve voltage-dependent rate constants. These states are (1) closed and activatable (resting); (2) open (activated); and (3) closed and nonactivatable (inactivated). Activation controls the rate and voltage dependence of the increase in intracellular sodium concentration following depolarization. Inactivation influences the rate and voltage dependence of positive potential returning to negative potential as the activated sodium channel returns to the resting level during maintained depolarization.[1,6]

The structural morphology of neuronal sodium channels is species and tissue dependent. For example, NVSC from eel electroplax consists of only a single α-subunit.[7] However, sodium channels from rat brain contain three polypeptides: (1) a 260 kDa α-subunit, (2) a 36 kDa β_1-subunit, and (3) a 33 kDa β_2-subunit,[1,5,8] with the α-subunit independently sufficient for functional expression.[5] Furthermore, sodium channels found in neurons have pharmacological and physiological properties different from those in skeletal muscle or cardiac cells.

NVSC subtypes from many species have been cloned, and amino acid sequences have been determined for examples from rat and human brain and skeletal and cardiac tissue.[4] For example, three major NVSC α-subunit isoforms from rat brain have been designated as type I, II, and III,[1] with each containing six α-helical transmembrane segments, although additional isoforms have more recently been described.[10]

The NVSC undergoes specific binding with neurotoxins, and at least seven neurotoxin binding sites have been identified.[11] Site 2 interacts with grayanotoxin and the alkaloids veratridine, aconitine, and batrachotoxin, resulting in persistent activation of the sodium channel. A batrachotoxin derivative, [^{3}H]batrachotoxinin A 20-α-benzoate ([^{3}H]BTX-B),[12−14] has been extensively used in in vitro radioligand binding assays for evaluating the interactions of small molecules with the NVSC. For example, the allosteric inhibition of [^{3}H]-BTX-B binding by the antimaximal electroshock (anti-MES) anticonvulsant diphenylhydantoin (phenytoin or DPH)[15] at therapeutically relevant concentrations (40 μM) first implicated the NVSC as a potential anticonvulsant receptor site.[16] Other classes of drugs also interact with the NVSC and inhibit [^{3}H]BTX-B binding, including the local anesthetics and antiarrhythmics. Consistently, these three classes of therapeutic agents often possess overlapping pharmacological activities, illustrated by the antiarrhythmic properties exhibited by both the anticonvulsant DPH and the local anesthetic lidocaine. Proposals for one-site[17] and two-site[18] models continue to provide controversy concerning whether anticonvulsants, local anesthetics, and antiarrhythmics act at either the same or different sites on the NVSC.

Interconversions between NVSC states may be important in considering the modes of action of these drugs. The distribution of channels among the three states, resting, opened, and inactivated, is a function of membrane potential and time.[19,20] Compounds that bind to the NVSC may, because of changes in access or interconversion rates, have different binding affinities to the resting, activated, or inactivated state of the sodium channel. This provides one possible explanation for the differences in binding and therapeutic profiles among anticonvulsants, local anesthetics, and antiarrhythmics.[21,22] DPH binds to the inactivated state of the NVSC in a voltage- and frequency-dependent manner,[23] providing an explanation for its selective effects on hyperactive versus normal neurons.

Examination of membrane effects for DPH using fluorescent fatty acid probes[24] implied that DPH may exert an inhibitory effect on the NVSC by simple

* Address correspondence to this author.
[†] Department of Chemistry.
[‡] Department of Psychiatry and Behavioral Neurobiology.
[⊗] Abstract published in *Advance ACS Abstracts,* January 15, 1997.

S0022-2623(96)00692-9 CCC: $14.00

partitioning into the lipid bilayer. However, DPH exhibits saturable binding to the NVSC, which is associated with properties of specific receptor−ligand interactions.[25] Studies[18] also indicate that sodium channel blockade by DPH is affected by changes in intracellular, but not extracellular, pH.

The effects of log *P*[26] and 5-phenyl ring orientation[27] on whole animal anticonvulsant activity have been summarized. Our preliminary investigations suggested that log *P*[28] and 5-phenyl ring orientation[29] may also be important for the efficient binding of hydantoins to the NVSC. Here we systematically evaluate the effects of log *P* and NVSC binding for a structurally diverse group of hydantoins **1**−**12** which possess a range of log *P* values (0.96−2.96). Within this group, we also make comparisons between structural isomers that vary 5-phenyl ring orientation while maintaining a constant log *P*.

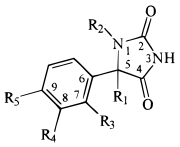

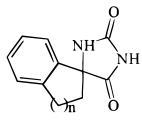

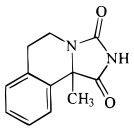

	R_1 (3′ 2′ 1′)	R_2	R_3	R_4	R_5
1	$CH_3CH_2CH_2$	H	H	H	H
2	$CH_3(CH_2)_2CH_2$	H	H	H	H
3	$CH_3(CH_2)_3CH_2$	H	H	H	H
4	$CH_3(CH_2)_2CH_2$	H	CH_3	H	H
5	$CH_3(CH_2)_2CH_2$	H	H	CH_3	H
6	$CH_3(CH_2)_2CH_2$	H	H	H	CH_3
7	CH_3	CH_3CH_2	H	H	H
DPH	Ph	H	H	H	H

	n
8	1
9	2
10	3
11	4

12

Methods

Biological Data. All compounds **1**−**12** were evaluated for relative binding to the NVSC (Table 2) in an in vitro assay using rat cerebral cortex synaptoneurosomes. Results are expressed as log IC_{50}, where IC_{50} represents the micromolar concentration of compound required to inhibit the specific binding of [^{3}H]BTX-B by 50%.

Conformational Analysis. All compounds were energy minimized with the Tripos force field[30] (SYBYL software) using default bond distances and angles and neglecting electrostatics. While all compounds were synthesized and evaluated as racemic mixtures, for internal consistency the geometries of **1**−**12** were modeled in SYBYL using only the arbitrarily chosen *R*-configuration at C5. Conformational searching was utilized to estimate the energetically reasonable range of torsion angles (N1,C5,C6,C7) for rotation of the phenyl ring relative to the hydantoin ring.

For **1**−**7** we performed, using GRIDSEARCH, conformational searches of torsion angle N1,C5,C6,C7 rotated 0−179° (for symmetrical phenyl rings in **1**−**3** and **5**−**7**) or 0−359° (for the unsymmetrical phenyl ring in **4**) in 1° increments. Briefly, GRIDSEARCH utilizes a torsion angle driver followed by energy minimization (Tripos force field). For **1**−**6** the starting position of the R_1 group was fully extended with an N1,C5,-C1′,C2′ torsion angle of 50°. After viewing the results, selected conformations near each apparent local energy minimum were submitted to an additional minimization to confirm that the local energy minimum had been identified. For compound **4**, selected conformations with energies roughly 2 kcal/mol above the global minimum were also energy-minimized after first defining the N1,C5,C6,C7 atoms as a rigid aggregate (to fix the N1,C5,C6,C7 torsion angle); this procedure more accurately defined the range of torsion angles within 2 kcal/mol of the global minimum. The results revealed that, for analogs **1**−**3** and **5**−**7**, all conformations from 0 to ±180° are within 2 kcal/mol of the lowest energy minimum. A single energy minimum was found for all but **7**, whose two minimum energy conformations placed the methyl of the *N*-ethyl group either above (**7a**) or below (**7b**) the plane of the hydantoin ring. In contrast, for compound **4**, higher rotational energy barriers were observed, and two torsion angle ranges of phenyl ring conformers were identified within 2.0 kcal/mol of the lowest energy minimum (Table 2). The lowest energy minimum within each range positioned the *o*-methyl group either above (**4a**) or below (**4b**) the plane of the phenyl ring. For DPH the conformation of the X-ray crystal structure[31] was used. Other than the torsion angles of the phenyl groups (see footnote *k* in Table 2), the calculated torsion angles, bond angles, and bond lengths for DPH were in close agreement with those of the crystal structure.

Conformational searches on rotationally restricted 5-phenyl analogs **8**−**12** were performed using RANDOM SEARCH. In this approach all bonds that are part of the aliphatic ring, except the fusion bond shared with the benzene ring (and the hydantoin ring for **12**), were selected for searching. The method sets up to three of the selected bonds to random torsional angles, and the resulting conformer is submitted to energy minimization to locate the nearest local minimum. The minimization is performed in two stages so that molecules with energy higher than a cutoff value (the default value of 70 kcal/mol was used) are eliminated early. The second stage of minimization uses gradient termination to ensure complete minimization. The resulting conformer is then compared to all previous structures based upon an RMS match of the atoms; if different, it is retained. The other default values utilized were 1000 maximum perturbation/minimization cycles, an RMS threshold of 0.2 Å (the minimum difference between two conformations to be designated as unique), a convergence threshold of 0.005, and six maximum hits (the number of times each unique conformer must be identified to terminate the search). Each search was repeated, starting with a different conformer, to verify results. Table 2 reports all minima whose energies were within 2 kcal/mol of the global minimum.

To estimate phenyl torsion angle ranges within 2 kcal/mol of the lowest energy conformer for **8**−**12**, each local energy minimum was evaluated in the following manner. The bond connecting the alkyl ring fragment to the phenyl ring was removed, the N1,C5,C6,C7 torsion angle was rotated by 5°, and the bond was reconnected. Atoms N1, C5, C6, and C7 were defined as an aggregate (fixing the torsion angle), and the resulting conformer was energy-minimized. This was performed in each direction (+ and −) from the local energy minimum until a conformer was generated whose energy was 2 kcal/mol greater than the global energy minimum. The results are given in Table 2.

Chemistry

The syntheses of analogs **1**−**3**,[28] **7**,[29] **8**,[32] **9**,[29] **10**−**11**,[33] and **12**[29] were previously described. In the preparation of hydantoin **11**,[33] we synthesized benzocylooctenone[34] by literature methods, and this was converted to **11** in 30% yield via synthetic method B (see the Experimental Section). New hydantoins **4**, **5**, and **6** were also prepared by the Bucherer-Berg[35] procedure from the appropriate ketones.[36] The starting ketones were synthesized using Grignard reactions of *o*-, *m*-, and *p*-tolyl nitrile and butylmagnesium bromide. Table 1 contains selected data for the compounds prepared in this study.

Results and Discussion

The neuronal voltage-sensitive sodium channel is a site of action for the anticonvulsant diphenylhydantoin, one of the most widely used agents for the treatment of generalized seizures. Unfortunately, the exact location and nature of this site has not yet been determined. We have been interested in investigating structure−activity relationships for the interactions of hydantoins with the NVSC in order to define structural features that give

Table 1. Selected Properties for Hydantoins **1**−**12**

compd	% isolated yield (method)	mp, °C
1	64 (A)	169−171 (165−166)[a]
2	65 (C)	204−205 (204−205)
3	91 (A)	119−122 (125−127)
4	20 (A)	144−145
5	56 (A)	162−164
6	60 (A)	158−160
7[b]	54	176−177
8	31 (A)	238−240 (238−240)
9[b]	91	240−242
10	51 (C)	250−255 (252−253)
11	30 (B)	201−202 (201−202)
12[b]	54	154−156

[a] Numbers in parentheses are literature melting ranges: **1**−**3**, **11** (ref 35); **8** (ref 32); **10** (ref 33). [b] Data previously reported in ref 29.

rise to efficient binding.[28,29] This approach may lead to new anticonvulsants with enhanced activity.

Previous investigations revealed that log *P* may be important for whole animal anticonvulsant activity,[26] and our preliminary studies suggested that both log *P* and phenyl ring orientation may be important for in vitro binding to the NVSC.[28,29] In the present study we have selected hydantoin analogs which provide more systematic evaluations for each of these properties.

We conveniently estimated log *P* values for new compounds, as we did in an earlier study,[28] by the addition of π values to the experimentally determined log *P* of the appropriate parent structure. We thus estimated the log *P* values in Table 2 for compounds **4**−**12** (the others were taken from ref 8) by adding the π values for substituents at C5 and N1 to the log *P* for 5-phenylhydantoin (0.46)[26] to provide the final log *P*. The π values used were 0.50 for each CH_2 or CH_3 in the alkyl chain at C5 and 0.56 for an N-CH_3 substituent.[37] For example, the log *P* for hydantoin **7** was calculated as $(\log P_{\text{parent}} + \pi_{5-\text{methyl}} + \pi_{\text{N1}-\text{methylene}} + \pi_{\text{methyl}}) = (0.46 + 0.50 + 0.56 + 0.50) = 2.02$. Since the ring closure of **7** provides the bicyclic hydantoin **12**, the log *P* of **12** was calculated as $(\log P_{\mathbf{7}} + \pi_{\text{ring closure}}) = 2.02 + (-0.50) = 1.52$.

We previously observed that structurally similar 5-alkyl-5-phenylhydantoin homologs **1**−**3** demonstrated enhanced binding to the NVSC with increases in log *P*.[28] However, as shown in Table 2, log *P* is not the only important variable. Comparisons of structurally dissimilar hydantoins with the same log *P* (e.g., **1** vs **7**, **2** vs **11**, **9** vs **12**) demonstrate that, in addition to log *P*, structural features influence the potency of binding to the NVSC. This is further supported by the observation that compounds **2** and **11**, which have log *P* values equivalent to that for DPH, do not exhibit comparable binding potencies. The linear correlation of log *P* versus sodium channel binding (log IC_{50}) for **1**−**12** and DPH (Figure 1) is only a moderately good model ($r^2 = 0.64$). This result indicates that simple nonspecific partitioning of hydantoins into the membrane lipid phase, which has been suggested by others as a possible mechanism for the effect of DPH on the NVSC,[24] is not sufficient for potent inhibition.

In a preliminary study we reported the NVSC binding of **1** vs **9** and **7** vs **12**, and the results suggested that the 5-phenyl orientation may be important for the in vitro binding of hydantoins to the NVSC.[29] To further investigate the effects of 5-phenyl orientation, independent from the effects of log *P*, we designed, synthesized, and evaluated NVSC binding for new hydantoins **4**−**6** and we also prepared and evaluated known spirohydantoins **8**−**11** and tricyclic hydantoin **12**. Compounds **4** and **8**−**12** all contain phenyl rings with more restricted energetically favorable rotameric conformations as compared to **1**−**3**, **5**, and **6**. Compounds **5** and **6** serve as isomeric models of **4** that do not experience significant changes in phenyl ring conformational accessibility as compared to **1**−**3**.

To estimate the 5-phenyl ring orientations that are most highly populated in **1**−**12**, the torsional angles N1,-C5,C6,C7 for all minimum energy conformers within 2 kcal/mol of the lowest energy minimum were calculated. Around each energy minimum, the range of N1,C5,C6,-C7 torsional angles that provided conformations with energies ≤2 kcal/mol greater than the global energy minimum was also calculated. As illustrated in Table 2, all phenyl ring orientations of compounds **1**−**3** and **5**−**7** meet the above criterion, while compound **4** exhibits one large and one narrow torsional angle range. Compounds **8**−**11** represent a homologous series of spirohydantoins containing phenyl rings that are conformationally restricted about N1,C5,C6,C7 due to a 5-alkyl side chain that is covalently bound to the *ortho* position of the 5-phenyl ring, and the range of accessible torsion angles defining the 5-phenyl conformations increases for larger ring sizes. Compound **12** is much more highly constrained.

One notes in Table 2 that the sodium channel binding activity increases in going from **8**−**10**, with no further increase in activity for **11**. One possible explanation for this trend is that increases in log *P* may correlate with increased binding activity. However, an exception is evident in that compound **11**, which exhibits a larger log *P* than **10**, does not exhibit a corresponding increase in sodium channel binding activity. Another possible explanation for this trend is the inability of the 5-phenyl substituent of the smaller ring systems to adopt a preferred conformation. A comparison between hydantoins with identical log *P* values from the spiro series (**8**−**11**) and the least restricted series (**1**−**3**) reveals that **1** exhibits roughly the same IC_{50} as **10** and that **2** exhibits roughly the same IC_{50} as **11**, suggesting that **10** and **11** may each be able to adopt an optimum phenyl ring orientation.

To further pursue this question, we prepared and evaluated the isomeric series **4**−**6**, for which all examples have the same log *P*. These compounds were designed to have the same log *P* value (2.96) as the most potent compound in this study, hydantoin **3**. In this series the *o*-methyl group of **4** restricts phenyl ring orientation as compared to isomers **3**, **5**, and **6**. Note that even though log *P* is constant, there is a 5.8-fold range in the sodium channel IC_{50} values. Interestingly, compounds **3**, **5**, and **6** all exhibit potent binding to the NVSC as compared to compound **4** (Table 2). This suggests that compound **4** may not be able to significantly populate the phenyl ring conformation required for optimum sodium channel binding activity.

Table 2. Conformational Analysis Results, Lipophilicities, and Sodium Channel Binding Activities for Hydantoins **1**−**12** and DPH

hydantoin[a]	torsion angle range, deg N1,C5,C6,C7[b]	low-energy conformer torsion angle, deg N1,C5,C6,C7[c]	energy, kcal/mol[d]	log *P*	Na^+ channel IC_{50} (μM)
1	0 to ±180	4	7.8	1.96 (2.10)[f]	162[e] [136−193][g]
2	0 to ±180	4	8	2.46 (2.63)	103[e] [85−124]
3	0 to ±180	4	8.1	2.96 (3.16)	39[e] [32−47]
4a	−108 to 1	−37	11	2.96 (3.08)	225 [218−233]
4b	147−169	159	12		
5	0 to ±180	4	8.2	2.96 (3.13)	58 [57−60]
6	0 to ±180	4	8.2	2.96 (3.13)	95 [86−106]
7a	0 to ±180	−42	7	2.02	720[n]
7b		−57	7	(−)[h]	
8a	89−159	144	15	0.96 (0.91)	2112 [2021−2207]
8b		104	15		
9a	95−158	138	8.1	1.46 (1.47)	851[i] [761−953]
9b		115	8.2		
10a	67−102	87	14.3	1.96 (2.03)	251 [225−280]
10b	107 − (−177)	163	13.7		
10c		135	15		
10d		118	15		
10e		152	15		
10f		107	16		
11a	83−178	153	20	2.46 (2.59)	251 [228−277]
11b		118	20		
12a	−4 to 26	11	9.3	1.52 (−)[h]	250[n]
12b	32−42	37	10.9		
DPH	0 to ±180	2[j]	7.1[k]	2.46[l] (2.08)	40[m]

[a] Letters in parentheses designate different low-energy conformers when more than one was identified. [b] The range of torsion angles calculated to be within 2 kcal/mol of the lowest energy minimum. [c] The lowest energy conformation(s) within the indicated torsion angle range. [d] Calculated using the Tripos Force Field (Maximin2) within SYBYL 6.1 and neglecting electrostatics. [e] The sodium channel binding data was taken from ref 28. [f] For comparison, numbers in parentheses are log *P* values calculated by the ClogP for Windows 1.0.1 program distributed by BioByte Corp. of Claremont, CA. [g] Range describing −1 to +1 standard deviation. [h] Could not be calculated by ClogP due to a missing fragment value. [i] The sodium channel value was determined in the present study. [j] Taken from the X-ray crystal structure in ref 31. [k] The energy calculated for the x-ray structure. The energy calculated for the minimized structure (Tripos force field) (N1,C5,C6,C7 torsion angle = −11°) was similar (6.9 kcal/mol). [l] The experimental value from ref 37. [m] Reference 15. [n] Reference 29.

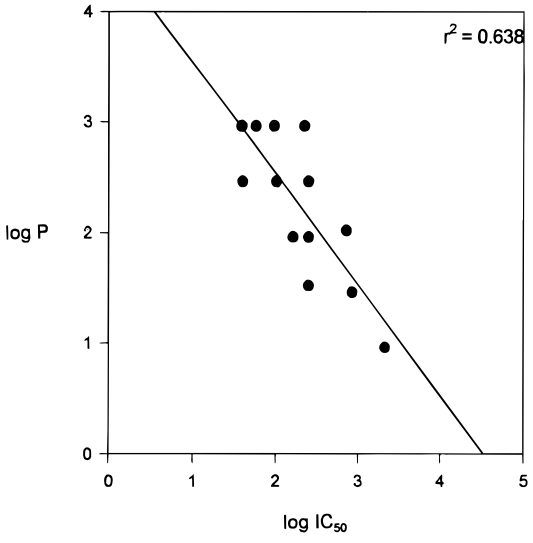

Figure 1. A linear correlation of log *P* versus sodium channel binding activity for hydantoins **1**−**12** and DPH.

Besides structurally similar hydantoins **3**−**6** (log *P* = 3), the compounds in Table 1 can also be divided into three distinct groups of hydantoins which contain structurally dissimilar compounds exhibiting the same log *P* values. In comparing **9** and **12** (log *P* = 1.5), IC_{50} changes 3.4-fold; for **1**, **7**, and **10** (log *P* = 2), IC_{50} changes 4.4-fold; for **2**, **11**, and DPH (log *P* = 2.5), IC_{50} changes 6.3-fold. Within each group the minimum energy conformation for the most potent examples contain phenyl ring torsion angles (N1,C5,C6,C7) of −11 to 11°. Energy minima for the least potent compounds contain considerably different phenyl ring torsion angles. These results suggest an optimum phenyl torsional angle range.

In conclusion, log *P* is clearly an important parameter for the potent binding of hydantoins to the NVSC. This may result from the necessity of hydantoins to enter or cross the cell membrane prior to interaction with the channel protein. However, the above studies, which compare structurally diverse hydantoins with identical log *P*, reveal that different hydantoins with the same log P value may exhibit significantly different binding affinities, suggesting that hydantoins likely bind to a specific site on the NVSC. Furthermore, these results suggest a preferred phenyl ring orientation that gives rise to the optimum binding of 5-phenylhydantoins to this site.

Experimental Section

Melting points were recorded on an Electrothermal melting point apparatus and are uncorrected. IR spectra were recorded on a Beckman Acculab 6 and Nicolet IR/42 spectrometers, and elemental analyses were performed by Atlantic Microlabs of Norcross, GA. ^{1}H NMR and ^{13}C NMR spectra were recorded on GE (NT series) and Bruker (ARX series) NMR spectrometers operating at 300.1 MHz (for ^{1}H). The spectra were obtained in DMSO-d_6 (for hydantoins) and $CDCl_3$ (for all other compounds) at ambient temperature and referenced internally to tetramethylsilane (TMS). Mass spectra were obtained on a Hewlett-Packard 5885 GC/MS. Spectral data for new hydantoins **4**−**6** are summarized below.

[^{3}H]Batrachotoxinin A 20-α-benzoate ([^{3}H]BTX-B) with a specific activity of 30 Ci/mol was obtained from New England Nuclear (Boston, MA).

Method A. To a stirring solution of 50% ethanol were added ketone (0.66 mol/L), KCN (1.33 mol/L) and $(NH_4)_2CO_3$ (2.66 mol/L). The solution was warmed to 50−65 °C for 12 h. After the solution was cooled to room temperature, the hydantoin precipitate was filtered, and the filtrate was acidified (pH 2) by the addition of concentrated HCl to give more precipitate, which was filtered again. The filtrate was concentrated to half-volume and cooled, and the hydantion product that precipitated was filtered. The solids were combined and recrystallized from hot ethanol to give the final product.

Method B. To a solution of 50% ethanol contained in a 300 mL Parr pressure apparatus were added ketone (0.7 mol/L), KCN (1.3 mol/L), and $(NH_4)_2CO_3$ (2.7 mol/L). The solution was heated at 125 °C for 24 h, the apparatus was cooled to room temperature, and the hydantoin precipitate was collected by filtration. The filtrate was adjusted to pH 2, concentrated to half-volume, cooled, and the hydantoin precipitate was filtered. The crude solids were combined and recrystallized in hot ethanol to give the final hydantoin product.

Method C. Ketone and trimethylsilyl cyanide (TMSCN) were combined without solvent in a 1:2 molar ratio under anhydrous conditions, and ZnI_2 (5−10 mg) was added as a catalyst. This mixture was stirred at room temperature under a nitrogen atmosphere for 12 h. The reaction was monitored by the disappearance of the C=O stretching peak in the IR spectrum of the reaction mixture. The TMS ether was not purified but was directly hydrolyzed to the cyanohydrin by adding equal amounts of ether and 15% HCl and stirring vigorously at room temperature for 1 h.[38] The ether layer was separated, and the acidic layer was washed three times with ether. The ether extracts were combined and evaporated to give cyanohydrin in 100% yield. The cyanohydrin was converted to hydantoin[35] by dissolving cyanohydrin and $(NH_4)_2CO_3$ in a 1:2 molar mixture in 50% ethanol. The mixture was then heated at 55−65 °C for 12 h. The reaction mixture was adjusted to pH 2 by the addition of HCl, concentrated to half-volume, and cooled, and the hydantoin precipitate was filtered. The crude solid was recrystallized from hot ethanol to give the final hydantoin product.

5-Butyl-5-(2-methylphenyl)hydantoin (4). To a solution of 50% ethanol (80 mL) contained in a 300 mL Parr pressure apparatus were added 1-(2-methylphenyl)pentanone (1.5 g, 8.5 mmol), KCN (1.1 g, 17 mmol), and $(NH_4)_2CO_3$ (3.9 g, 34 mmol). The solution was heated at 125 °C for 24 h, and the apparatus was cooled to room temperature. The precipitate was filtered, and the filtrate was acidified (pH 2) by the addition of concentrated HCl. The filtrate was concentrated to half-volume, cooled in an ice bath, and filtered again. The combined solids were recrystallized from hot ethanol to give pure **4** (0.50 g, 20% yield): mp 144-145 °C; ^{1}H NMR (DMSO-d_6) δ 7.42−7.36 (m, 2H, Ph), 7.21−7.15 (m, 2H, Ph), 6.44−6.38 (s, 1H, NH), 2.35−2.33 (s, 3H, CH_3), 2.24−1.98 (m, 2H, CH_2), 1.41−1.19 (m, 4H, CH_2), 0.90−0.84 (m, 3H, CH_3); ^{13}C NMR (DMSO-d_6) δ 177.0, 157.0, 137.0, 132.6, 128.2, 127.4, 126.1, 67.5, 36.7, 25.2, 22.3, 20.4, 14.1; IR (KBr) 1760, 1700 (C=O) cm^{-1}; MS (EI) 246 (M^+). Anal. ($C_{14}H_{18}N_2O_2$) C, H, N.

5-Butyl-5-(3-methylphenyl)hydantoin (5). To a stirring solution of 50% ethanol (30 mL) were added 1-(3-methylphenyl)pentanone (3.2 g, 18 mmol), KCN (2.4 g, 36 mmol) and $(NH_4)_2CO_3$ (8.3 g, 73 mmol). The solution was warmed to 50−60 °C for 48 h. After cooling to room temperature, the precipitate was filtered and the filtrate was acidified (pH 2) by the addition of concentrated HCl. The filtrate was concentrated to half-volume, cooled, and filtered again. The combined solids were recrystallized from hot ethanol to give pure **5** (2.5 g, 56% yield): mp 162−164 °C; ^{1}H NMR (DMSO-d_6) δ 7.42−7.36 (m, 2H, Ph), 7.21−7.15 (m, 2H, Ph), 6.44−6.38 (s, 1H, NH), 2.35−2.33 (s, 3H, CH_3), 2.24−1.98 (m, 2H, CH_2), 1.41−1.19 (m, 4H, CH_2), 0.90−0.84 (m, 3H, CH_3); ^{13}C NMR (DMSO-d_6) δ 175.9, 157.6, 138.5, 137.6, 129.1, 128.7, 125.9, 122.3, 68.9, 38.5, 25.8, 22.5, 21.6, 13.8; IR (KBr) 1750, 1705 (C=O) cm^{-1}; MS (EI) 246 (M^+). Anal. ($C_{14}H_{18}N_2O_2$) C, H, N.

5-Butyl-5-(4-methylphenyl)hydantoin (6). To a stirring solution of 50% ethanol (30 mL) were added 1-(4-methylphenyl)pentanone (2.6 g, 15 mmol), KCN (1.9 g, 30 mmol), and $(NH_4)_2CO_3$ (6.7 g, 59 mmol). The solution was warmed to 50−60 °C for 48 h. After the solution was cooled to room temperature, the precipitate was filtered, and the filtrate was acidified (pH 2) by the addition of concentrated HCl. The filtrate was concentrated to half-volume, cooled, and filtered again. The combined solids were recrystallized from hot ethanol to give pure **6** (2.1 g, 60% yield): mp 158−160 °C; ^{1}H NMR (DMSO-d_6) δ 7.42−7.36 (m, 2H, Ph), 7.21−7.15 (m, 2H, Ph), 6.44−6.38 (s, 1H, NH), 2.35−2.33 (s, 3H, CH_3), 2.24−1.98 (m, 2H, CH_2), 1.41−1.19 (m, 4H, CH_2), 0.90−0.84 (m, 3H, CH_3); ^{13}C NMR (DMSO-d_6) δ 175.5, 156.7, 138.3, 134.6, 129.6, 125.1, 68.8, 38.3, 25.8, 22.5, 21.0, 13.8; IR (KBr) 1710, 1700 (C=O) cm^{-1}; MS (EI) 246 (M^+). Anal. ($C_{14}H_{18}N_2O_2$) C, H, N.

Sodium Channel Binding Assay. We previously reported the details of this procedure.[39] Briefly, synaptoneurosomes (~1 mg of protein) from rat cerebral cortex were incubated for 40 min at 25 °C with the test compound (seven different concentrations spanning the IC_{50}) in a total volume of 320 μL containing 10 nM [^{3}H]BTX-B and 50 μg/mL of scorpion venom. Incubations were terminated by dilution with ice-cold buffer and filtration through a Whatman GF/C filter paper, and the filters were washed four times with ice-cold buffer. Filters were counted in a Beckmann scintillation counter. Specific binding was determined by subtracting the nonspecific binding, which was measured in the presence of 300 μM veratridine, from the total binding of [^{3}H]BTX-B. All experiments were performed in triplicate and included a control tube containing 40 μM DPH. The IC_{50} values were determined from a Probit analysis of the dose−response curve and excluded doses producing less than 10% or greater than 90% inhibition.

Acknowledgment. This work was taken in part from the Ph.D. dissertation submitted in partial fulfillment of the requirements for the Ph.D. degree in chemistry by M.L.B. M.L.B gratefully acknowledges financial support from the Patricia Robert Harris Fellowship, the National Consortium for Educational Access, the UAB Comprehensive Minority Faculty Development Program, and the UAB Department of Chemistry. We also thank Ms. Bereaval Webb, a 1993 Alabama Alliance for Minority Participation (AMP) summer intern, for technical support.

References

(1) Catterall, W. A. Structure and Function of Voltage-Gated Ion Channels. *Annu. Rev. Biochem*. **1995**, *64*, 493−531.
(2) Kirsch, G. E. Na^+ Channels: Structure, Function, and Classification. *Drug Dev. Res*. **1994**, *33*, 263−276.
(3) Catterall, W. A. Molecular Mechanisms of Inactivation and Modulation of Sodium Channels. *Renal Physiol. Biochem*. **1994**, *17*, 121−125.
(4) Kallen, R. G.; Cohen, S. A.; Barchi, R. L. Structure, Function and Expression of Voltage-Dependent Sodium Channels. *Mol. Neurobiol*. **1993**, *7*, 383−428.
(5) Catterall, W. A. Structure and Function of Voltage-Sensitive Ion Channels. *Science* **1988**, *242*, 50−61.
(6) Armstrong, C. M. Voltage-Dependent Ion Channels and Their Gating. *Physiol. Rev*. **1992**, *72*, S5-S13.

(7) Noda, M.; Shimizu, S.; Tanabe, T.; Takai, T.; Kayano, T.; Ikeda, T.; Takahashi, H.; Nakayama, H.; Kanaoka, Y.; Minamino, N.; Kangawa, K.; Matsu, H.; Raftery, M. A.; Hirose, T.; Inayama, S.; Hayashida, H.; Miyata, T.; Numa, S. Primary Structure of *Electrophorus-Electricus* Sodium Channel Deduced from Complementary DNA Sequence. *Nature* **1984**, *312*, 121−127.
(8) Scheuer, T.; Auld, V. J.; Boyd, S.; Offord, J.; Dunn, R.; Catterall, W. A. Functional Properties of Rat Brain Sodium Channels Expressed in a Somatic Cell Line. *Science* **1990**, *247*, 854−858.
(9) Black, J. A.; Westenbroek, R.; Ransom, B. R.; Catterall, W. A.; Waxman, S. G. Type II Sodium Channels in Spinal Cord Astrocytes In Situ: Immunocytochemical Observations. *Glia* **1994**, *12*, 219−227.
(10) George, A. L., Jr.; Varkony, T. A.; Drabkin, H. A.; Han, J.; Knops, J. F.; Finley, W. H.; Brown, G. B.; Ward, D. C.; Haas, M. Assignment of Human Heart Tetrodotoxin-Resistant Voltage-Gated Na+ Channel α-Subunit Gene (SCN5A) to Band 3p21. *Cytogenet. Cell Genet.* **1995**, *68*, 67−70.
(11) Fainzilber, M.; Kofman, O.; Zlotkin, E.; Gordon, D. A New Neurotoxin Receptor Site on Sodium Channels is Identified by a Conotoxin that Affects Sodium Channel Inactivation in Molluscs and Acts as an Antagonist in Rat Brain. *J. Biol. Chem.* **1994**, *269*, 2574−2580.
(12) Catterall, W. A.; Morrow, C. S.; Daly, J. W.; Brown, G. B. Binding of Batrachotoxinin A 20-α-Benzoate to a Receptor Site Associated with Sodium Channels in Synaptic Nerve Ending Particles. *J. Biol. Chem.* **1981**, *10*, 8922−8927.
(13) Brown, G. B.; Tieszen, S. C.; Daly, J. W.; Warnick, J. E.; Albuquerque, E. X. Batrachotoxin-A 20-α-Benzoate: A New Radioactive Ligand for Voltage-Sensitive Sodium Channels. *Cell Mol. Neurobiol.* **1981**, *1*, 19−40.
(14) Brown, G. B. Batrachotoxin: A Window on the Allosteric Nature of the Voltage-Sensitive Sodium Channel. *Int. Rev. Neurobiol.* **1988**, *29*, 7−116.
(15) Willow, M.; Catterall, W. A. Inhibition of Binding of [^{3}H]-Batrachotoxinin A 20-α-Benzoate to Sodium Channels by the Anticonvulsant Drugs Diphenylhydantoin and Carbamazepine. *Mol. Pharmacol.* **1982**, *22*, 627−635.
(16) Catterall, W. A. Common Modes of Drug Action on Na^+ Channels: Local Anesthetics, Antiarrhythmics and Anticonvulsants. *Trends Pharmacol. Sci.* **1987**, *8*, 57−65.
(17) Zimányi, I.; Weiss, S. R. B.; Lajtha, A.; Post, R. M.; Reith, M. E. A. Evidence for a Common Site of Action of Lidocaine and Carbamazepine in Voltage-Dependent Sodium Channels. *Eur. J. Pharmacol.* **1989**, *167*, 419−422.
(18) Barber, M. J.; Starmer, C. F.; Grant, A. O. Blockade of Cardiac Sodium Channels by Amitriptyline and Diphenylhydantoin, Evidence for Two Use-Dependent Binding Sites. *Circ. Res.* **1991**, *69*, 677−696.
(19) Koumi, S.; Sato, R; Katori, R.; Hisatome, I.; Nagasawa, K.; Hayakawa, H. Sodium Channel States Control Binding and Unbinding Behavior of Antiarrhythmic Drugs in Cardiac Myocytes for the Guinea Pig. *Cardiovasc. Res.* **1993**, *26*, 1199−1205.
(20) Courtney, K. R.; Etter, E. F. Modulated Anticonvulsant Block of Sodium Channels in Nerve and Muscle. *Eur. J. Pharmacol.* **1983**, *88*, 1−9.
(21) Catterall, W. A. Inhibition of Voltage-Sensitive Sodium Channels in Neuroblastoma Cells by Antiarryhthmics Drugs. *Mol. Pharmacol.* **1981**, *20*, 356−362.
(22) Catterall, W. A. Inhibition of Voltage-Sensitive Sodium Channels in Neuroblastoma Cells and Synaptosomes by the Anticonvulsant Drugs Diphenylhydantoin and Carbamazepine. *Mol. Pharmacol.* **1984**, *25*, 228−234.
(23) Catterall, W. A. Voltage Clamp Analysis of the Inhibitory Actions of Diphenylhydantoin and Carbamazepine on Voltage-Sensitive Sodium Channels in Neuroblastoma Cells. *Mol. Pharmacol.* **1985**, *27*, 549−558.
(24) Harris, W. E.; Stahl, W. L. Interactions of Phenytoin with Rat Brain Synaptosomes Examined by Flourescent Fatty Acid Probes. *Neurochem. Int.* **1988**, *13*, 369−377.
(25) Francis, J.; Burnham, W. M. [^{3}H]Phenytoin Identifies a Novel Anticonvulsant-Binding Domain on Voltage-Dependent Sodium Channels. *Mol. Pharmacol.* **1992**, *42*, 1097−1103.
(26) Lien, E. Structure-Activity Correlations for Anticonvulsant Drugs. *J. Med. Chem.* **1970**, *13* ,1189−1191.
(27) Wong, M. G.; Defina, J. A.; Andrews, P. R. Conformational Analysis of Clinically Active Anticonvulsant Drugs. *J. Med. Chem.* **1986**, *29*, 562−572.
(28) Brouillette, W. J.; Jestkov, V. P; Brown, M. L.; Aktar, M. S.; Delorey, T. M.; Brown, G. B. Bicyclic Hydantoins with Bridgehead Nitrogen. Comparison of Anticonvulsant Activities with Binding to the Neuronal Voltage-Dependent Sodium Channel. *J. Med. Chem.* **1994**, *37*, 3289−3293.
(29) Brouillette, W. J; Brown, G. B.; Delorey, T. M; Liang, G. Sodium Channel Binding and Anticonvulsant Activities of Hydantoins Containing Conformationally Constrained 5-Phenyl Substituents. *J. Pharm. Sci.* **1990**, *79*, 871−874.
(30) Vinter, J. G.; Davis, A.; Saunder, M. R. Strategic Approaches to Drug Design. 1. An Integrated Software Framework for Molecular Modeling. *J. Comput.-Aided Mol. Des.* **1987**, *1*, 31−55.
(31) Camerman, A.; Camerman, N. The Stereochemical Basis of Anticonvulsant Drug Action. I. The Crystal and Molecular Structure of Diphenylhydantoin, a Noncentrosymmetric Structure Solved by Centric Symbolic Addition. *Acta Crystallogr.* **1971**, *B27*, 2205−2211.
(32) Sarges, R.; Schnur, R. C.; Belletire, J. L.; Peterson, M. J. Spiro Hydantoin Aldose Reductase Inhibitors. *J. Med. Chem.* **1988**, *31*, 230−243.
(33) Huisgen, R.; Ugi, I. Polycyclische Systeme mit Heteroatomen. *Liebigs Ann. Chem.* **1957**, *610*, 57−66.
(34) Huisgen, R; Rapp, W.; Mitteil, I. 1,2-Benzo-cycloocten-(1)-on-(3)*. *Chem. Ber.* **1952**, *85*, 826−835.
(35) Novelli, A.; Lugones, Z. M.; Velasco, P. Hydantoins III. Chemical Constitution and Hypnotic Action. *An. Asoc. Quim. Argent.* **1942**, *30*, 225−231.
(36) Cazes, B; Julia, S. Rèarrangements Sigmatropiques [2.3] en Sèrie Benzylique; Prèparation de Cetones Ortho-Mèthyl-Arylèes. ([2,3] Sigmatropic Rearrangements of a Benzylic Series; Preparation of Ortho-methyl Aryl Ketones.) *Tetrahedron* **1979**, *35*, 2655−2660.
(37) Lipinski, C. A.; Giese, E. F.; Korst, R. J. pKa, Log P and MedChem CLOGP Fragment Values of Acidic Heterocyclic Potential Bioisosteres. *Quant. Struct.-Act. Relat.* **1991**, *10*, 109−117.
(38) Grunewald, G. L.; Brouillette, W. J.; Finney, J. Synthesis of α-Hydroxyamides via the Cyanosilylation of Aromatic Ketones. *Tetrahedron Lett.* **1980**, *21*, 1219−1220.
(39) Brouillette, W. J; Brown, G. B.; Delorey, T. M; Shirali, S. S. ; Grunewald, G. L. Anticonvulsant Activities of Phenyl-Substituted Bicyclic 2,4-Oxazolidinediones and Monocyclic Models. Comparison with Binding to the Neuronal Voltage-Dependent Sodium Channel. *J. Med. Chem.* **1988**, *31*, 2218−2221.

JM960692V